[13] R. J. Schilling, *Fundamentals of Robotics: Analysis and Control*. Englewood Cliffs, NJ: Prentice-Hall, 1990.
[14] R. Smith and P. Cheeseman, "On the estimation and representation of spatial uncertainty," *Int. J. Robot. Res.*, vol. 5, no. 4, 1987.
[15] F. L. Lewis, *Optimal Estimation*. New York: Wiley, 1986.
[16] H. F. Durrant-Whyte, "Consistent integration and propagation of disparate sensor observations," *Int. J. Robot. Res.*, 1987.
[17] A. C. Sanderson, "Cooperative navigation among multiple mobile robots," *Distributed Autonomous Robotic Systems II*, H. Asami, Ed. Tokyo, Japan: Springer-Verlag, 1996.

A High Integrity IMU/GPS Navigation Loop for Autonomous Land Vehicle Applications

Salah Sukkarieh, Eduardo M. Nebot, and Hugh F. Durrant-Whyte

***Abstract*—This paper describes the development and implementation of a high integrity navigation system, based on the combined use of the Global Positioning System (GPS) and an inertial measurement unit (IMU), for autonomous land vehicle applications. The paper focuses on the issue of achieving the integrity required of the navigation loop for use in autonomous systems. The paper highlights the detection of possible faults both before and during the fusion process in order to enhance the integrity of the navigation loop. The implementation of this fault detection methodology considers both low frequency faults in the IMU caused by bias in the sensor readings and the misalignment of the unit, and high frequency faults from the GPS receiver caused by multipath errors. The implementation, based on a low-cost, strapdown IMU, aided by either standard or carrier phase GPS technologies, is described. Results of the fusion process are presented.**

***Index Terms*—Autonomous systems, global positioning system, inertial measurement unit, Kalman filter, navigation.**

I. Introduction

The commercial development of large autonomous land vehicles in applications such as open-cast mining, agriculture and cargo handling requires the corresponding development of high integrity navigation (localization) systems. Such systems are necessary to provide knowledge of vehicle position and trajectory and subsequently to control the vehicle along a desired path. The need for integrity in such systems is paramount: undetected, erroneous, position or trajectory data can lead to catastrophic failure of the autonomous vehicle.

A growing number of research groups around the world are developing autonomous land vehicle systems for various applications (see [2], [4]–[6], and [13] for example). However, few of these works make explicit the essential need for system integrity that will be necessary in any future commercial development of this technology. Further, while many systems use Global Positioning System (GPS) and inertial technology, there has been no real application to understand, quantify and overcome the issue of failure and integrity in navigation systems based on these sensor technologies. This paper specifically addresses this issue in the context of autonomous land vehicle applications.

The focus of this paper is on the implementation of fault detection techniques that increase the integrity of the inertial measurement unit (IMU)/GPS navigation loop for land vehicle applications. The implementation processes adopted follows a decentralized data fusion philosophy and have been developed to ensure modularity. This ensures that the ability of the loop to detect the occurrence of faults is not prejudiced by the specific accuracy of the IMU or GPS sensors employed. This paper begins in Section II by providing the essential background on IMU and GPS sensor technologies in the context of sensor faults and the sensors specifically used in this paper. Section III presents the IMU error model implemented which forms the basis of the Kalman filter state model. Section IV focuses on faults, their nature and the means of detection in IMU and GPS systems. The nature of these faults and the means for detecting them are described. Section V details the implementation of this system with respect to the tuning of the filter and the resulting error growth. Section VI presents the vehicles used to test the loop along with the effect of the environment on the sensors. Finally, Section VII provides a series of experimental results that demonstrate the accuracy and integrity of the resulting system. Conclusions are then provided.

II. Sensors

The accuracy of the navigation loop is dependent on the accuracy of the IMU and GPS sensors implemented. The greater the accuracy of these sensors, the greater the accuracy of the overall navigation loop. Brief descriptions of IMU and GPS sensors follow. For further detail on IMU's refer to [3] and [11]. For GPS refer to [9].

A. IMU

The primary advantage of using an IMU on outdoor land vehicles is that the acceleration, angular rotation and attitude data is provided at high update rates. Thus the velocity and position of the vehicle can also be evaluated. Unlike wheel encoders, an IMU is not affected by wheel slip, which is encountered by the majority of land vehicle applications. There are however disadvantages to using an IMU. The errors caused by bias in the sensor readings accumulate with time and inaccurate readings are caused by the misalignment of the unit's axes with respect to the local navigation frame. These errors will be discussed in Section IV-A.

The IMU implemented in this work comprises of three accelerometers, three gyros and two pendulum gyros. These sets of sensors provide the acceleration, rotation rate and tilt of the vehicle respectively, in the body frame, at a frequency of 84 Hz.

B. GPS

The GPS receiver is an external or absolute sensor, thus the errors in the data it provides are bounded. However, the GPS unit is a low frequency sensor, thus providing the state information at low update rates. There are two forms of accurate GPS receiver technologies implemented in this work: standard differential and carrier phase differential. High frequency faults arise when the GPS signals undergo multipath errors. These errors occur when the GPS signal is reflected off one or more surfaces before it reaches the receiver antenna. This results in a longer time delay of the signal and hence affects the fix of the standard differential receiver and also alters the phase of the signal thus affecting the carrier phase

Manuscript received June 26, 1998; revised February 16, 1999. This paper was recommended for publication by Associate Editor K. Valavanis and Editor V. Lumelsky upon evaluation of the reviewers' comments.

The authors are with the University of Sydney, Sydney NSW 2006, Australia (e-mail: salah@mech.eng.usyd.edu.au; nebot@mech.eng.usyd.edu.au; hugh@mech.eng.usyd.edu.au).

Publisher Item Identifier S 1042-296X(99)03917-8.

differential fix. Another high frequency fault, although it occurs less often and with less effect, is when the receiver utilizes a different set of satellites in order to determine the position fix. The accuracy of the fix is dependent on the geometry of the observed satellites. Changes in satellite configuration due to blockages of the satellite view will in turn alter the resulting fix. Both forms of high frequency faults cause abrupt jumps in the position and velocity fixes obtained by the GPS receiver.

High frequency faults are therefore environment dependent. An open area such as a quarry will less likely produce multipath errors as will a container terminal. Consequently, the tuning of the filter which fuses the IMU and GPS data is dependent on the environment.

Even with the constant improvement of hardware and software in GPS technology [8], [12], multipath errors will remain. Only improvements in rejecting the worst cases have been accomplished. Slight multipath errors still occur, and a small error of half a meter is significant when using 0.02 m accuracy.

This work utilizes both the standard and carrier phase differential systems. The Ashtech G12 is used as the standard differential system, delivering a position accuracy of 1.5 m and 0.02 m/s in velocity at 10 Hz. The carrier phase differential system is obtained by using the Novatel RT receivers. An accuracy of 0.2 m and 0.02 m for position is obtained using the RT20 and RT2, respectively. Both provide 0.02 m/s accuracy in velocity. The data is transmitted at 4 Hz.

III. Fusion

The core of the navigation loop is a Kalman filter which estimates the position, velocity and attitude errors of the IMU. It accomplishes this by utilizing the GPS observations in order to determine these errors which are then used to correct the IMU.

A. Error Model

Due to the small velocities encountered by many land vehicles, Coriolis and transport rate terms are ignored along with any gravity anomalies. The velocity, position and attitude error propagation equations can then be written as [7], [11]

$$\delta \dot{v}_n = A_n \times \psi_n + C_b^n \delta A_b \tag{1}$$

$$\delta \dot{p}_n = \delta v_n \tag{2}$$

$$\delta \dot{\psi}_n = -C_b^n \delta \omega_b \tag{3}$$

where δA_b and $\delta \omega_b$ are the uncertainties in the accelerometers and gyros in the body frame (subscript b) which are then transformed over to the navigation frame (subscript n) using a direction cosine matrix (C_b^n) [10]. These errors are a summation of the individual errors which include bias, scale factors, misalignments, and nonlinearities. Each of these errors can be placed in the state model to be estimated. For example the bias in the accelerometers can be modeled as constant errors and the bias in the gyros as Markov processes such that

$$\dot{b}_{A_n} = b_{A_n}$$
$$\dot{b}_{\omega_n} = -\beta b_{\omega_n}.$$

However many land vehicles undergo constant stop and start maneuvers. During this stationary period, calibration can be employed and hence evaluation of the biases can be obtained with great accuracy. Thus the state model remains as represented in (1) to (3)

$$\begin{bmatrix} \delta \dot{p}_n \\ \delta \dot{v}_n \\ \delta \dot{\psi}_n \end{bmatrix} = \begin{bmatrix} 0 & I & 0 \\ 0 & 0 & A_n \\ 0 & 0 & 0 \end{bmatrix} \begin{bmatrix} \delta p_n \\ \delta v_n \\ \psi_n \end{bmatrix} \tag{4}$$

where I is a 3×3 identity matrix and A_n is the acceleration in the navigation frame represented in a skew-symmetric form. The error model is then incorporated in a standard linear Kalman filter implementing the prediction and estimation stages.

IV. Fault Detection

The correctable faults associated with the IMU/GPS navigation loop are classified into two groups: the low frequency faults caused by bias on the sensor readings within the IMU and the errors associated with the unit's misalignment, and the high frequency faults due to multipath errors in the GPS observations.

A. IMU Faults

The acceleration and rotation rate measured by the accelerometers and gyros respectively is represented as

$$A_i = A_{i_T} + b_{A_i} + \nu \tag{5}$$

$$\text{and} \quad \omega_i = \omega_{i_T} + b_{\omega_i} + \nu \tag{6}$$

where A_i is the measured acceleration of the ith accelerometer, A_{i_T} is the true acceleration that should be measured by the accelerometer and b_{A_i} is the bias found on this accelerometer. The same notation is used for the gyros. ν represents white noise.

The incremental velocity, position and rotation is then obtained by integrating (5) and (6)

$$V_i = V_{i_T} + b_{A_i} t + \int \nu \, dt \tag{7}$$

$$P_i = P_{i_T} + \frac{b_{A_i} t^2}{2} + \iint \nu \, dt \tag{8}$$

$$\theta_i = \theta_{i_T} + b_{\omega_i} t + \int \nu \, dt. \tag{9}$$

As presented in (7)–(9), the bias in the sensors play a major role in causing drift in the velocity, position and attitude information provided by the unit. Namely, the bias terms affect the velocity and attitude linearly with time, and the position quadratically.

As presented in [10] the gyro data is used to update the direction cosine matrix C_b^n. As a result, any drift in angle data caused by the integration of the gyro outputs will perturb the direction cosine matrix, causing erroneous acceleration values. By assuming that there is no bias or noise in the accelerometers, no noise in the gyros and that there is no angular rotation measured, then if the z-gyro has a constant bias, the acceleration error of the accelerometer along the X-axis will be

$$A_x = A_{x_T} \sin(b_{\omega_z} t).$$

For small angle increments

$$\begin{aligned} A_x &= A_{x_T} b_{\omega_z} t \\ \text{thus} \quad V_x &= \frac{1}{2} A_{x_T} b_{\omega_z} t^2 \\ \text{and} \quad P_x &= \frac{1}{6} A_{x_T} b_{\omega_z} t^3. \end{aligned} \tag{10}$$

Hence a bias in the gyro will cause an error in the position determination which will grow with the cube of time. Consequently, the biases on the gyros play an important role in causing drift in the position and velocity evaluations. The biases are obtained each time the vehicle is stationary in order to counteract the changing bias values due to temperature fluctuations. Alternatively the bias can be estimated and applied on-line. However, in the current applications the vehicles undergo frequent stopping. During this time the unit is calibrated, providing excellent results due to the quality of the pendulum gyros.

The removal of bias in the sensors does not however provide perfect solutions. This is due to the integration of white noise $(\int \nu \, dt)$ which places a growing error term on the sensors known as Random

Walk as presented in (7) and (9). Thus it is not evident what error value is present at any particular moment. However the standard deviation of the error due to unity Gaussian white noise at any particular moment in time is ([10])

$$\sigma_\nu = \sqrt{t}. \tag{11}$$

B. GPS Faults

The innovation covariance matrix in the Kalman filter, represents the uncertainty with the innovation, which in turn reflects the uncertainty in the observed error of the IMU. $\mathbf{R}(\mathbf{k})$ is the observation covariance matrix and represents the noise added to the innovation covariance $\mathbf{S}(\mathbf{k})$ during each observation. This matrix is the uncertainty in the GPS fix and hence in the accuracy of the GPS receiver. However, high frequency faults pose a problem. When an abrupt jump in the GPS fix occurs, the magnitude of the observation error will differ largely from the true error. This is reflected in the estimated error that is evaluated. The correction which results will cause the IMU to incorrectly follow these jumps in the GPS solution. Thus before an estimate can be obtained the observation needs to be validated. The chi-squared distribution test provides a validation process which utilizes the theoretical properties of the unbiasedness and whiteness of the innovation sequence

$$\mathbf{z}^{\mathbf{T}}(\mathbf{k})\mathbf{S}^{-1}(\mathbf{k})\mathbf{z}(\mathbf{k}) \leq \varsigma. \tag{12}$$

Equation (12) is a gating function that describes the probability concentration under Gaussian assumptions. The value ς is determined prior to the fusion process and represents the percentage probability that a particular observation lies within an ellipsoid [1]. Once the innovation and its associated covariance are obtained, the gating function is implemented, and if the result is less than or equal to ς, then the observation is accepted and the estimate proceeds. Due to satellite geometry, the GPS fix in the vertical plane is significantly less accurate than that in the horizontal plane. Thus the fix in North and East may lie well within the validation region, whilst that of Down may exceed it and force the result of the gating function beyond the gamma threshold. Thus a ς is chosen to best suit the environment and the probability region allowed, but by also taking into consideration that although a larger ς will include the vertical fix, it will also accept erroneous horizontal fixes. To apply more stringent rules to the fault detection routine each observation element should be validated individually. Thus if a fault is detected in any state the whole observation is discarded.

The value of ς is usually set to reject innovations exceeding the 95% threshold. Apart from rejecting the erroneous fixes caused by multipath, the gating function allows the filter to remain optimal.

During the rejection of multipath errors, the fusion process remains at the prediction stage, and subsequently, the IMU is not corrected. Thus the risk of the IMU wandering off and missing all GPS fixes is apparent. As a result, the tuning process of the filter is a crucial step in the fusion implementation. The process noise matrix, which represents the inherent inaccuracy of the unit along with the confidence in its calibration and alignment, needs to be tuned so that the covariance grows at a rate quick enough to grasp the first available GPS fix. This is described in the following section.

V. Tuning Implementation

There are two stages in the filter flow, namely the prediction stage where the predicted IMU errors are always zero and the uncertainty in such a solution grows with time, and the estimation stage where the estimates of the IMU errors are obtained by placing a weighting on the observation. This poses a problem if no observation is obtained for an extended period of time or if the GPS fixes are rejected due to errors. During these cases the filter will remain in the prediction stage and no errors will be evaluated to correct the IMU. Due to the error characteristics of the IMU this will cause a drift in the states evaluated by the IMU. The longer the duration of no correction, the greater the correction on the IMU once a GPS fix is used, which will then cause large jumps in the IMU indicated states.

As with any Kalman filter process, tuning lies with what values to place in the state covariance matrix $(\mathbf{Q})$ and the observation covariance matrix $(\mathbf{R})$. A large $\mathbf{Q}$ will imply an inaccurate IMU error model. During the prediction stage the uncertainty in the IMU data will grow according to the amount of noise injected. Hence when a GPS fix does occur there is a greater possibility the IMU will be corrected using the first available GPS fix irrespective of the accuracy of this fix. Likewise small $\mathbf{R}$ values will imply accurate GPS fixes and result in a similar situation. Furthermore, a large $\mathbf{Q}$ value will cause the IMU to closely follow the GPS fixes. If the GPS fixes have high uncertainty and hence are noisy, then the corrected IMU will also be noisy. This is particularly important when implementing low accuracy GPS units.

Tuning is a delicate adjustment of both the $\mathbf{Q}$ and $\mathbf{R}$ matrices along with the employment of the gating function (12), in order to reject the high frequency faults of the GPS.

Section IV-B discusses how to determine the variances in the observation matrix $\mathbf{R}$. Determining the values for the state covariance matrix $\mathbf{Q}$ depends on the source of the noise being considered. The major cause of the errors in the IMU is bias. If these errors are modeled as white noise then the accuracy of such an implementation depends on the length of time between two calibrations which in turn depends on the application. It is necessary to ensure that the window of time between two calibrations is small enough to account for all rates of change. Otherwise the biases need to be modeled.

The principle tuning parameters which need to be addressed are the velocity and attitude values. Placing large uncertainty in the velocity terms will imply greater reliance on the GPS velocity fixes which should be implemented if one can guarantee excellent velocity fixes. This is due to the fact that the velocity terms are reflected in both the position and attitude evaluations. Furthermore, the more accurate the velocity terms the greater the dampening on the attitude errors. Large uncertainties in the attitude values however cause oscillatory corrections in attitude thus causing the attitude to oscillate as well . The tuning procedure required for the velocity and attitude values in order to obtain reliable results is delicate.

VI. Experimental Setup

A. Vehicles

The navigation loop was implemented on a number of land vehicles. These include a utility (Fig. 1) and a straddle carrier (Fig. 2). The distinct advantage of implementing this navigation loop is the ease with which the sensors are mounted onto the vehicles.

B. Environment

The utility was driven in an open area with occasional building and tree foliage whereas the straddle carrier is located in a container terminal at a port. The containers which the straddle carrier has to pick up are lower than the vehicle. Thus by mounting the GPS aerial on top of the straddle carrier no multipath errors will occur from these containers. However, as the straddle carrier passes alongside a quay crane, multipath errors will occur. Furthermore, if the straddle carrier passes under the crane then total satellite blockage will occur. Hence fault detection techniques in a port environment are particularly important.

Fig. 1. The utility is one of the test vehicles implemented and is primarily used as a test bed for the sensors.

Fig. 2. Position and orientation of a 65 ton straddle carrier in a port is determined using the IMU/GPS navigation loop.

VII. Results

A. Alignment

Fig. 3 presents the fused data using the 0.02 m position and 0.02 m/s velocity GPS technology onboard the utility. The GPS delivers fixes at 4 Hz while the IMU sampling rate is at 84 Hz. Hence between any two GPS fixes there are a minimum of twenty IMU samples. This infers that the prediction cycle of the Kalman filter runs twenty times faster than the estimation cycle. Fig. 4 is an enhanced view of the vehicle on two occasions when the vehicle's initial heading was incorrect by five degrees. The bottom path portrays the vehicle slightly after it has begun its journey while the top path presents the vehicle on the return. The on-line alignment of the IMU has corrected this error by the time the vehicle returns to the final position.

Fig. 5 is an enhanced view of the velocity of the vehicle at the final stage of the test. Without any on-line alignment of the IMU the resulting velocity of the vehicle at the end of the run is presented in Fig. 6. The velocity in Fig. 6 has a prominent saw-tooth characteristic as compared to Fig. 5. This is due to the offset in the acceleration. Between GPS fixes this offset in acceleration causes the velocity of the vehicle to deviate before being corrected by the next GPS fix.

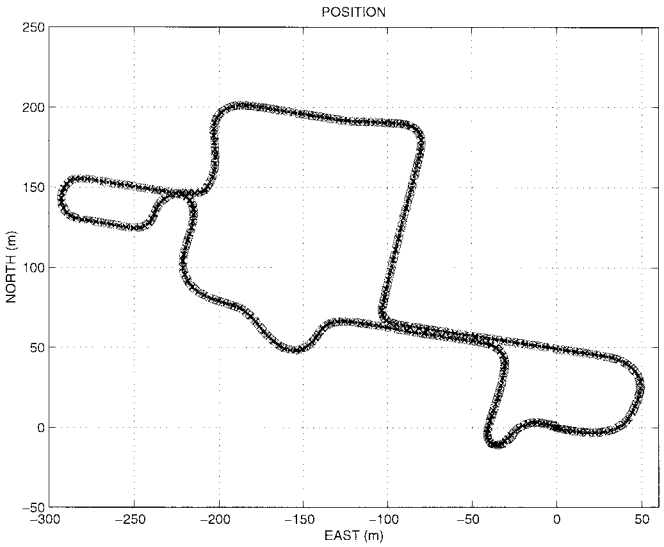

Fig. 3. Fusion result using the 0.02 m position and 0.02 m/s velocity technology.

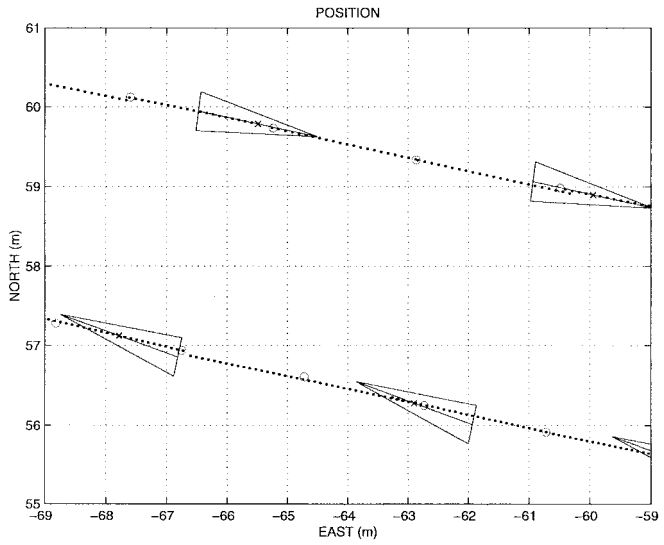

Fig. 4. Enhanced view of the area showing the heading of the vehicle after an initial error is placed on the heading. The heading is corrected by the time the vehicle returns.

The offset in the acceleration is due to the inaccurate computed Pitch angle of the vehicle. Thus, Figs. 4 and 5 demonstrate how important the on-line alignment is.

B. GPS Fault Detection

Fig. 7 presents the fused result of the navigation loop onboard a straddle carrier at a port. This result implements the 1.5 m position, 0.02 m/s velocity GPS sensor. The GPS provides fixes at 10 Hz hence there are approximately eight prediction cycles per estimation cycle. The vehicle starts in position 0 m *North*, 0 m *East* and moves in a counter clockwise direction. The vehicle firstly passes around some containers before approaching a crane indicated in the lower right portion of the figure. As the vehicle approaches the crane multipath errors occur until the vehicle reaches a stage where the GPS receiver cannot locate any more satellites because the vehicle is under the crane. At this stage no GPS fixes occur. As the vehicle departs from beneath the crane, slight multipath errors still occur. The multipath

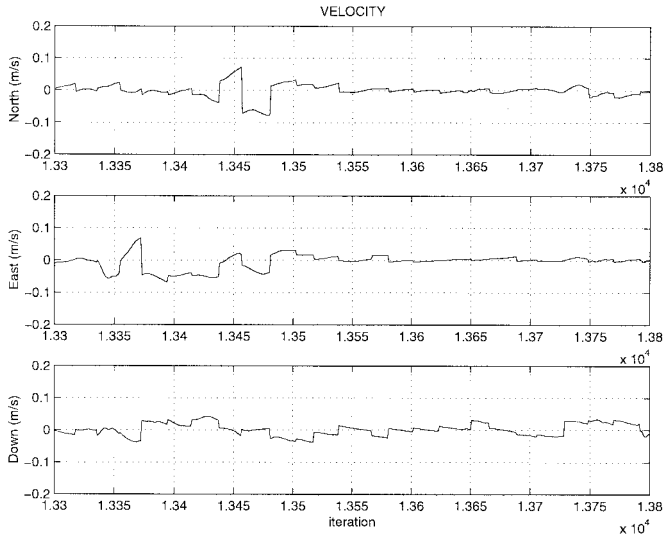

Fig. 5. Enhanced view of the velocity of the vehicle at the end of the run **with** attitude correction.

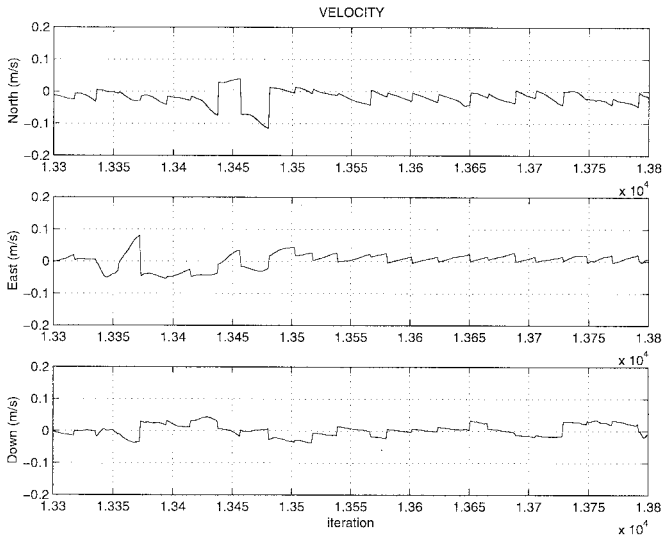

Fig. 6. Enhanced view of the velocity of the vehicle at the end of the run **without** attitude correction.

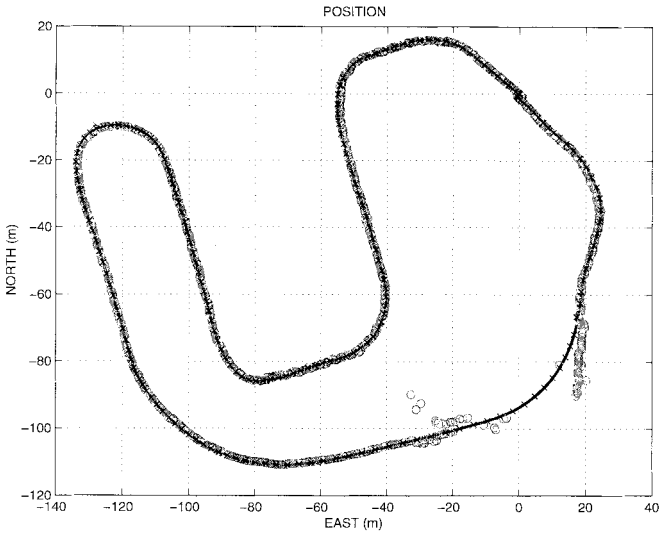

Fig. 7. Position of the straddle carrier as it maneuvers around containers before driving under a quay crane.

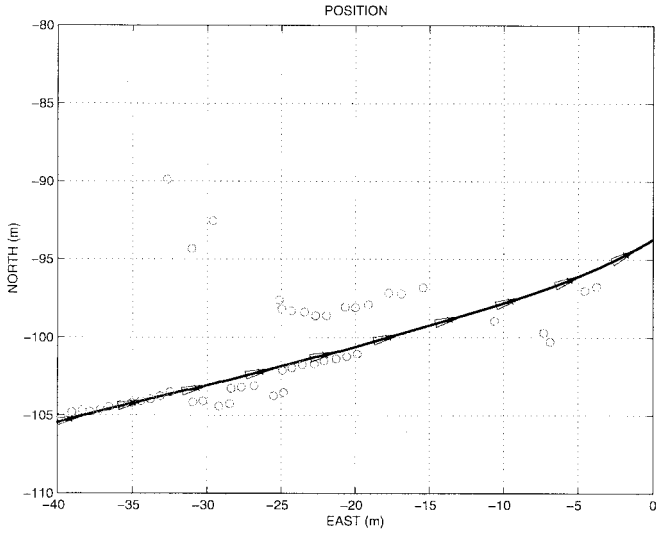

Fig. 8. Before the vehicle approaches the crane multipath errors occur. These GPS fixes, however, have been detected as faults and hence are not used as observations and the IMU is not inaccurately corrected.

errors stop once the vehicle has reached the position -68 m *North*, 18 m *East*. Fig. 8 is an enhanced view of this faulty region. The filter rejects the incorrect GPS fixes until the end of the faulty region where there is a slight adjustment since the uncertainty in the IMU solution is, at this stage, greater than that of the GPS fix. During the faulty portion of the trajectory the filter remains in the prediction stage and the IMU runs alone. Furthermore the on-line alignment algorithm has aligned the IMU such that the unit is accurate to complete the path whilst there are no GPS fixes. During tuning greater accuracy was placed on the velocity observations as compared to the position observations. The values used are the position and velocity accuracies as determined by the specifications of the GPS unit.

Fig. 9 presents the fused result with the same tuning parameters however with no multipath rejection. Without fault rejection the innovations not only exceed the two sigma bound but the fused result closely follows the GPS fixes, creating a noisy fusion result. The filter can be tuned so as to place less weighting on the observations. This is accomplished by increasing the accuracy of the model by placing smaller covariances in the $\mathbf{Q}$ matrix. Fig. 10 presents the fused result with such an implementation and Figs. 11 and 12 are the corresponding position and velocity innovations. Although Fig. 10 would closely resemble the true fusion result, the innovations judge it to be unacceptable. By not implementing any GPS fault detection techniques not only is the filter sub-optimal since the innovations lie beyond the two sigma bound, but incorrect error estimates will be obtained. Thus if for some reason the GPS was shut off during the multipath region the IMU would have been inaccurately corrected and proceeded with incorrect states which is detrimental to the integrity of the system.

VIII. Conclusion

With the realization of the potential for many land service vehicles to become either semi or fully autonomous the need for highly accurate, reliable and robust navigation systems need to be developed. This is where the IMU/GPS navigation loop discussed in this paper fits into all three categories.

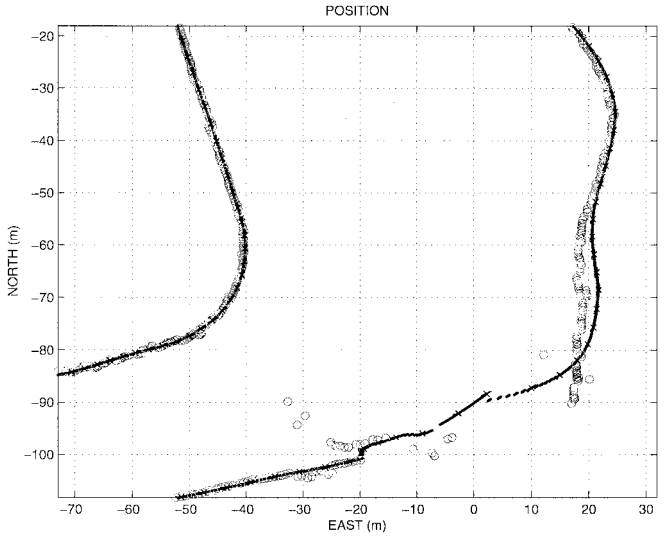

Fig. 9. With the same tuning parameters, however, with no fault detection routines the IMU closely follows the GPS multipath errors.

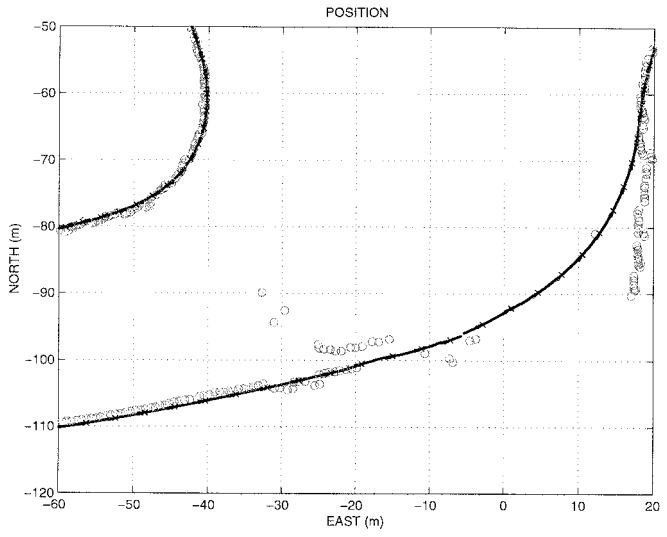

Fig. 10. With no GPS fault detection, the path of the vehicle can be made to resemble the true path by placing greater accuracy in the state model and hence in the IMU. Thus less weighting is placed on the GPS fixes.

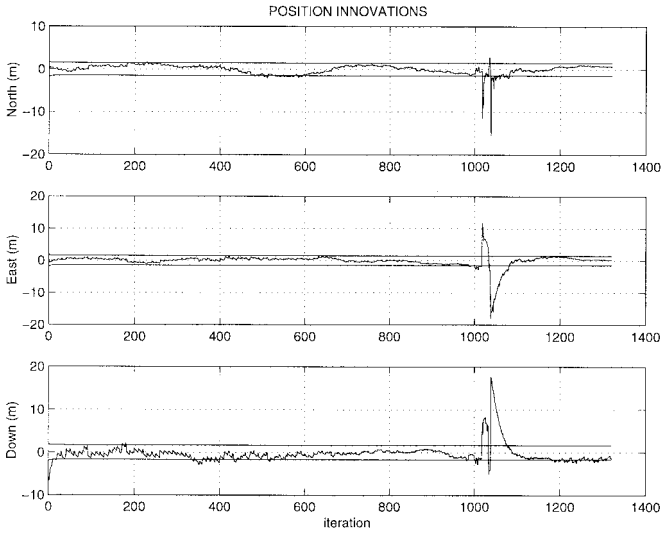

Fig. 11. The position innovations show that the filter is behaving sub-optimally even when it is tuned to place little emphasis on the GPS fixes.

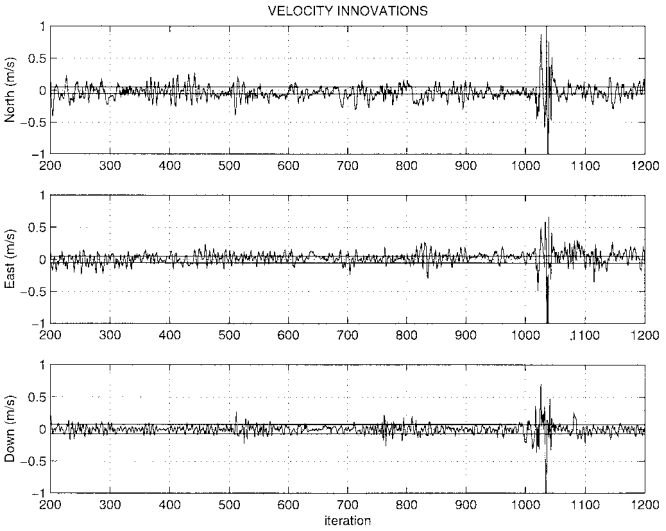

Fig. 12. The velocity innovations further magnify the suboptimality of the filter when it is tuned to seemingly reject multipath errors.

The observable and correctable faults associated with this navigation loop were classified into two groups: the low frequency faults of the IMU; and the high frequency faults of the GPS sensor.

The low frequency faults were associated with the biases found in the accelerometers and gyros within the unit. However, due to the constant start and stop maneuvers which these land vehicles undertake, calibration of the unit during this period is all that is required to determine these biases. It was demonstrated that if the biases were not removed from the gyros, the position error would increase with the cube of time. However, even when the biases are removed, the integration of the noise on the sensors would cause drift in the evaluation of the states. Thus the GPS sensor is used to constantly correct the IMU and remove these errors.

The high frequency faults of the GPS are predominantly caused by the reflection of the signals from surrounding objects known as "multipath." Hence the GPS fixes have to be constantly monitored in order to determine if they are at fault. The validation procedure implemented uses the innovations and their associated covariances evaluated by the filter to determine the whiteness and unbiasedness of the innovations. It was stated that the GPS fixes do not have the same accuracy in the horizontal plane as they do in the vertical because of satellite geometry. Hence the validation was applied to each state separately in order to apply more stringent tests.

With fault detection applied to remove any inaccurate GPS fixes, the fusion of the two sensors not only corrects any errors in the IMU but also aligns the unit as the vehicle moves even if, as presented in the results, the initial heading of the vehicle is inaccurate.

Thus it has been shown that the IMU/GPS navigation loop is an ideal candidate for land vehicle applications if fault detection techniques and on-line alignment are implemented.

REFERENCES

[1] Y. Bar-Shalom and X. Li, *Estimation and Tracking—Principles, Techniques and Software*. Norwood, MA: Artech House, 1993.

[2] J. Borenstein, H. R. Everett, L. Feng, and D. Wehe, "Mobile robot positioning sensors and techniques," in *J. Robot. Syst.*, vol. 14, no. 4, pp. 231–249, 1997.

[3] K. R. Britting, *Inertial Navigation System Analysis*. New York: Wiley, 1971.
[4] R. Chatila, S. Lacroix, S. Betge-Brezetz, M. Devy, and T. Simeon, "Autonomous mobile robot navigation for planet exploration—The EDEN project," in *Proc. IEEE Int. Conf. Robot. Automat.*, 1996.
[5] G. Giralt, L. Boissier, and L. Marechal, "The Iares project: Rovers for the human conquest of the moon and Mars," in *Proc. IEEE Int. Conf. Robot. Automat.*, 1996.
[6] E. Krotkov, R. Simmons, F. Cozman, and S. Koenig, "Safeguarded teleoperation for lunar rovers: From human factors to field trials," in *Proc. IEEE Int. Conf. Robot. Automat.*, 1996.
[7] P. Maybeck, *Stochastic Models, Estimation and Control*. New York: Academic, 1982, vol. 1.
[8] NOVATEL Inc., *GPSCard*, Software Version 4.437, Hardware Version 3.05, Nov. 1996.
[9] B. W. Parkinson and J. J. Spiker, Jr., *Global Positioning System: Theory and Applications*. Washington, DC: American Institute of Aeronautics and Astronautics, Inc., 1996.
[10] S. Sukkarieh, E. M. Nebot, and H. Durrant-Whyte, "Achieving integrity in an INS/GPS navigation loop for autonomous land vehicle applications," in *Proc. IEEE Int. Conf. Robot. Automat.*, May 1998.
[11] D. H. Titterton and J. L. Weston, *Strapdown Inertial Navigation Technology*. Stevenage, U.K.: Peregrinus, 1997.
[12] F. Van Diggelen, *GPS and GPS + GLONASS RTK*, in ION-GPS, Sept. 1997.
[13] R. Volpe, J. Balaram, T. Ohm, and R. Ivlev, "The rocky 7 mars rover prototype," in *Proc. IEEE Int. Conf. Robot. Automat.*, 1996.

Sliding Mode Control for Trajectory Tracking of Nonholonomic Wheeled Mobile Robots

Jung-Min Yang and Jong-Hwan Kim

***Abstract*— Nonholonomic mobile robots have constraints imposed on the motion that are not integrable, i.e., the constraints cannot be written as time derivatives of some function of the generalized coordinates. The position control of nonholonomic mobile robots has been an important class of control problems. In this paper, we propose a robust tracking control of nonholonomic wheeled mobile robots using sliding mode. The posture of a mobile robot is represented by polar coordinates and the dynamic equation of the robot is feedback-linearized by the computed-torque method. A novel sliding mode control law is proposed for asymptotically stabilizing the mobile robot to a desired trajectory. It is shown that the proposed scheme is robust to bounded external disturbances. Experimental results demonstrate the effectiveness of accurate tracking capability and the robust performance of the proposed scheme.**

***Index Terms*—Nonholonomic wheeled mobile robots, sliding mode control, trajectory tracking.**

I. Introduction

It is known that stabilization of nonholonomic wheeled mobile robots with restricted mobility to an equilibrium state is in general quite difficult. A well-known work of Brockett [1] identifies nonholonomic systems as a class of systems that cannot be stabilized via smooth state feedback. It implies that problems of controlling nonholonomic systems cannot be applied to methods of linear control theory, and they are not transformable into linear control problems. Due to both their richness and hardness, such nonlinear control problems have motivated a large number of researches involving various techniques of automatic control. Another difficulty in controlling nonholonomic mobile robots is that in the real world there are uncertainties in their modeling. Taking into account intrinsic characteristics of mobile robots such as actual vehicle dynamics, inertia and power limits of actuators and localization errors, their dynamic equations could not be described as a simplified mathematical model. A survey of recent developments in control of nonholonomic systems is described in [2]. To the authors' knowledge, the problem of dealing with model uncertainties is one of research problems for nonholonomic systems that require much attention but have yet to be extensively studied. Among previous researches, Jiang and Pomet [3], [4] applied backstepping technique to the adaptive control of nonholonomic systems with unknown parameters. A controller robust against localization errors of nonholonomic mobile robots was proposed by Hamel et al. [5], which considered the parking problem of mobile robots. In [6], a robust path-following controller for mobile robots was proposed guaranteeing exponential stability.

As an approach for robust control, sliding mode control has been applied to the trajectory control of robot manipulators [7], [8], and is recently receiving increasing attention from researches on control of nonholonomic systems with uncertainties. The advantages of using sliding mode control include fast response, good transient performance and robustness with regard to parameter variations. Bloch and Drakunov [9] proposed a sliding mode control law for stabilizing a nonholonomic system expressed in chained form, and extended their work to tracking problems [10]. Guldner and Utkin [11], [12] proposed a Lyapunov navigation function to prescribe a set of desired trajectories for navigation of mobile robots to a specified configuration. They used sliding mode control to guarantee exact tracking of trajectories made by navigation functions. Chacal and Sira-Ramirez [13] developed a sliding mode control which exploits a property named differential flatness of kinematics of mobile robots. Aguilar et al. [14] presented a path-following feedback controller with sliding mode which is robust to localization and curvature estimation errors for a car-like robot.

While the above works are mainly based on kinematic models of nonholonomic systems, models that include dynamic effects are required for other purposes, for instance, using torques as control inputs. The approaches based on dynamic models of nonholonomic systems include the work of Su and Stepanenko [15], who developed a reduced dynamic model for simultaneous independent motion and force control of nonholonomic systems. They proposed a robust control law which is a smooth realization of sliding mode control. In Shim and Kim [16], a variable structure control law was proposed with which mobile robots converge to reference trajectories with bounded errors of position and velocity.

In this paper, we propose a novel sliding mode control law for solving trajectory tracking problems of nonholonomic mobile robots. Mobile robots with the proposed control law converge to a given reference trajectory with asymptotic stability. We use dynamic models of mobile robots to describe their behaviors with bounded disturbances in system dynamics. Specifically, posture variables of mobile robots represented in *polar coordinates* are used for designing appropriate sliding surfaces which stabilize all the posture variables. By means of the computed-torque method, error dynamics of mobile

Manuscript received March 24, 1998; revised March 23, 1999. This paper was recommended for publication by Associate Editor J. Wen and Editor A. De Luca upon evaluation of the reviewers' comments.

The authors are with the Department of Electrical Engineering, Korea Advanced Institute of Science and Technology (KAIST), Taejon-shi 305-701, Korea (e-mail: yjm@vivaldi.kaist.ac.kr; johkim@vivaldi.kaist.ac.kr).

Publisher Item Identifier S 1042-296X(99)04980-0.